Analysis of low-energy-electron diffraction intensity profiles from the (100) and (111) faces of copper*

G. E. Laramore
Sandia Laboratories, Albuquerque, New Mexico 87115
(Received 1 August 1973)

Low-energy-electron-diffraction (LEED) intensity profiles are calculated for the (100) and (111) faces of copper and compared with experimental measurements. Calculations using a self-consistent electron-ion-core potential due to Snow and Waber are compared with calculations using a potential constructed from a simple overlap of atomic charge densities. The differences are found to be inconsequential as far as analyzing LEED spectra. Five partial-wave components are used to describe the vibronically renormalized electron–ion-core elastic-scattering vertex. The value of the inner potential V_0 is determined by comparing the position of the Fermi level in Snow and Waber's band calculation with work-function measurements. Except for one set of data on the (111) face, this value of V_0 gives a good placement of peak positions for electron energies $\lesssim 240$ eV. It is found that the fine structure in the calculated profiles for the (111) face is considerably more sensitive to the value of the mean-free-path parameter used to describe the imaginary part of the one-electron self-energy than that in the calculated profiles for the (100) face. Analysis of the data indicates that the upper-layer spacing is the same as the bulk value (to within $\sim 5\%$) for both faces.

I. INTRODUCTION

In this paper the finite temperature version of the inelastic-collision model[1–5] is used to analyze experimental[6–8] low-energy-electron-diffraction (LEED) intensity profiles from the (100) and (111) faces of copper. The experimental measurements considered here cover the energy range between 0 and 240 eV for a reasonable range of angles of incidence. All of the measurements considered were made at room temperature ($T \simeq 300\,^{\circ}\mathrm{K}$). Although experimental data[9] showing the variation of the scattered intensity with temperature exist for Cu(100), they will not be considered in the present study.

In a previous work[5] LEED intensity profiles from Ni(100) and Ni(111) were analyzed using a muffin-tin potential constructed from a simple overlap of atomic charge densities. Here we compare intensity profiles calculated using a similarly constructed potential with those calculated using a self-consistent band-structure potential due to Snow and Waber.[10] The differences in the calculated intensity profiles are found to be insignificant as far as analyzing LEED spectra. This is important since the technique of constructing electron–ion-core potentials from overlapping atomic or ionic charge densities can be easily extended to the case of adsorbed overlayers[11] whereas it will probably be some time before self-consistent potentials are available for such systems. The value for the inner potential V_0 used in the calculations was obtained by comparing the experimental work function[12,13] for polycrystalline copper to the position of the Fermi level in Snow and Waber's[10] band calculation. Except for one set of data[8] on Cu(111), this value of V_0 gives an adequate placement of peak positions in the calculated intensity profiles. The imaginary part of the one-electron self-energy was parameterized in terms of a constant inelastic mean free path as was originally done by Duke and Tucker.[14] Initially a value of 8 Å was used for λ_{ee} since this value gave an adequate description of the scattering data from nickel[5] and it was felt that copper and nickel should not be too different in regards to this parameter. This value of λ_{ee} gave a good description of the scattering from Cu(100) but did not give an adequate description of the fine structure in the experimental profiles from Cu(111). Using $\lambda_{ee} = 11$ Å gave a much better description of this latter fine structure and gave only very small changes in the shapes of the calculated intensity profiles for Cu(100). Hence, it appears that the fine structure in the calculated curves for Cu(111) is more sensitive than that in the calculated curves for Cu(100) and presumably this observation will extrapolate to other fcc materials as well.

This paper augments previous calculations[15–19] of LEED intensities from copper which consider only a limited number of intensity profiles from Cu(100) that were taken at normal or nearly normal incidence. An earlier work by Laramore *et al.*[15] used Snow and Waber's potential[10] to describe the electron–ion-core scattering but because of the limitations of the computer code available at that time, used only the first three partial-wave components. Here we use five partial-wave components to describe the vibronically renormalized electron–ion-core scattering amplitude and the attendant improvement in describing the experimental data can be easily seen by comparing

the calculated curves in this paper with those in Ref. 15. The calculations of Jepsen, Marcus, and Jona[18,19] also use a band-structure potential to characterize the electron–ion-core interaction but the potential they use is due to Burdick.[20] In contrast with these calculations, Pendry[16,17] uses an electron–ion-core potential with the exchange coefficients especially modified for the high-energy range of LEED. The agreement between theory and experiment found in the present work is comparable with that found by Jepsen *et al.*[18,19] and appears somewhat better than that exhibited by Pendry.[16,17] The dependence of the calculated intensity profiles on small changes in the upper-layer spacing is investigated for the specular beam at selected angles of incidence and the results indicate that the upper-layer spacing is the same as the bulk value (to within ~5% or about 0.1 Å) for both faces.

In Sec. II the model used in the calculations is briefly described and calculated intensity profiles using the potential constructed from overlapping atomic charge densities are compared with those calculated using the potential of Snow and Waber.[10] In Secs. III and IV, respectively, model calculations of LEED intensity profiles are performed for Cu(100) and Cu(111) and compared with experimental measurements. Finally, in Sec. V we summarize our results.

II. DESCRIPTION OF MODEL

The basic equations defining the inelastic-collision model have been previously set forth[1–5] and so here we present only those which serve to define the parameters used in the calculation.

The first parameter that enters the calculation is that which describes the renormalization of the electron–ion-core elastic scattering amplitude by the lattice vibrations. Assuming a Debye model for the phonon spectrum, the effective electron–ion-core elastic-scattering vertex for the nth ion core can be written as[1,2]

$$b_n(\vec{k}_2,\vec{k}_1)=\exp[-W(T,\Theta_D^n,M_n)(\vec{k}_2-\vec{k}_1)^2]\times t_n(\vec{k}_2,\vec{k}_1)\ , \tag{1}$$

where

$$W(T,\Theta_D^n,M_n)=\frac{3\hbar^2}{2M_n k_B\Theta_D^n}\left[\frac{1}{4}+\int_0^{\Theta_D^n/T}dx\,\frac{x}{e^x-1}\right], \tag{2}$$

and $t_n(\vec{k}_2,\vec{k}_1)$ is the scattering amplitude for the nth ion core when it is held rigid. $t_n(\vec{k}_2,\vec{k}_1)$ is specified in terms of phase shifts obtained from the electron–ion-core model potential.[2,3] In Eq. (2) T is the temperature of the solid, M_n is the mass of the nth ion core, and Θ_D^n is the Debye temperature parameterizing the vibrational amplitude of the ion core. There is little doubt that the surface atoms have a larger amplitude of vibration than those in the bulk, but since we are dealing with only room-temperature data we shall use a value of $\Theta_D=343\,^\circ$K for both surface and bulk atoms.[21,22] The description of both the correct shapes of the intensity profiles and their temperature dependence is potentially a more involved task[23] which we will defer until after the room-temperature data are understood. Nevertheless, it is interesting to note that using a very simple model Holland[24] correctly described many interesting features of the temperature dependence of the experimental data[9] although he was forced to use angles of incidence other than those stated for the experimental curves. The particular algorithm that we employ to obtain the partial-wave components of $b_n(\vec{k}_2,\vec{k}_1)$ is the same one detailed in Ref. 5 with a total of five partial-wave components being used.

We use the simple model of the electronic self-energy first proposed by Duke and Tucker[14] and used with reasonable success in the past in LEED calculations for several different materials,[3,5,11,15,25] i.e., where

$$\Sigma(\vec{k},E)=\Sigma(E)=-V_0-i\Gamma(E)\ , \tag{3}$$

$$\Gamma(E)=\frac{\hbar^2}{m\lambda_{ee}}\left[\frac{2m}{\hbar^2}(E+V_0)\right]^{1/2}. \tag{4}$$

As in Ref. 5, we assume that the renormalization effects of the electronic self-energy start one-half an atomic-layer spacing outside the position of the outer-most plane of ion cores.

Muffin-tin potentials are used to determine $t_n(\vec{k}_2,\vec{k}_1)$ and we take V_0 to be the distance from the muffin-tin zero to the vacuum. The first muffin-tin potential that we consider is the self-consistent potential of Snow and Waber.[10] The calculated value of V_0 for this potential was 13.3 eV where a constant of integration was determined by forcing the 1s eigenvalue of the self-consistent potential to be equal to the 1s eigenvalue of the starting potential. Energy bands were calculated using this self-consistent potential and the Fermi level was found to lie 5.7 eV below the vacuum. This is about 1.1 eV deeper than work-function measurements for polycrystalline copper indicate–the measurements of Mitchell and Mitchell[12] give $\varphi=4.6$ eV, and the measurements of Riviere[13] give $\varphi=4.5$ eV. Thus, to be more consistent with work-function measurements we take $V_0=12.2$ eV in our calculation. It is interesting to note that if Snow and Waber[10] would not have required the 1s eigenvalues of their "self-consistent" potential and their starting potential to coincide, they would have obtained $V_0=12.0$ eV. The $l=0$–4 phase

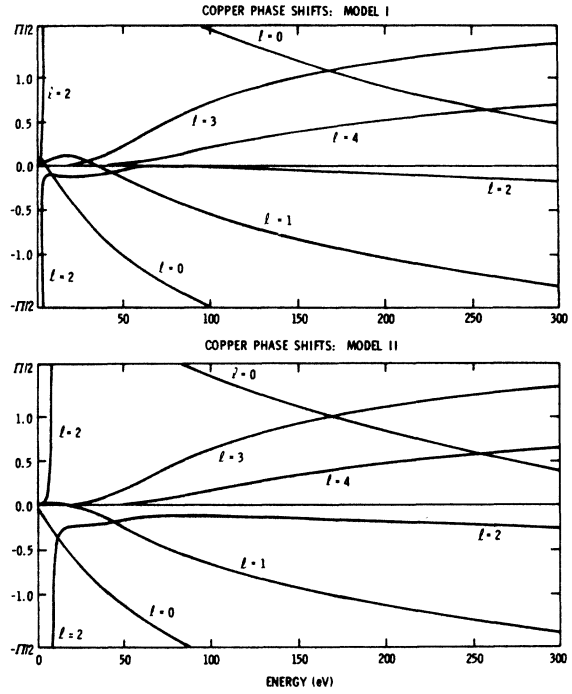

FIG. 1. Copper phase shifts for the potential models described in the text. Model I is the self-consistent potential of Snow and Waber (Ref. 10) and model II is the potential constructed from a simple overlap of atomic charge densities. In each case the energy scale is measured relative to the constant value of the potential between the muffin tins which was calculated to be 13.3 eV below the vacuum for model I and 14.6 eV below the vacuum for model II.

shifts for this potential are shown as model I in Fig. 1. We will use only these five phase shifts to model the electron–ion-core scattering. This gave a good description of the experimental LEED intensity profiles for nickel which is a material having a similar scattering strength.

The other muffin-tin potential that we consider was obtained from a simple overlap of atomic charge densities following conventional band-structure techniques. Atomic charge densities were obtained following the relativistic Hartree-Fock-Slater calculation of Liberman *et al.*[26] These atomic charge densities were overlapped and muffin-tin potential constructed following Loucks.[27] The Slater[28] local-exchange approximation

$$V_{\text{exch}}(r) = -6\alpha\left[\frac{3}{8\pi}\rho(r)\right]^{1/3} \tag{5}$$

was used with the Kohn-Sham[29] value of $\alpha = \frac{2}{3}$ in both the free-atom calculation and the muffin-tin construction. A three-dimensional perfect-crystal configuration was assumed in the potential construction with a lattice constant of 3.61 Å and a muffin-tin radius of 1.27 Å being used. The calculated value of V_0 for this potential was 14.6 eV. In the nickel work[5] it was found that the value of V_0 calculated according to this procedure was too large and it was adjusted using the d-wave resonance to locate the approximate center of gravity of the d band and hence the approximate position of the Fermi level. However, in copper the d band is completely filled and the Fermi level lies in the $4s$ band,[10] and so this procedure would be of little use. Since a complete band-structure calculation is outside the scope of the present work, we are forced either to treat V_0 as a completely adjustable parameter or to use the value of V_0 found for potential model I. The latter course was chosen in the subsequent calculations. The $l = 0$–4 phase

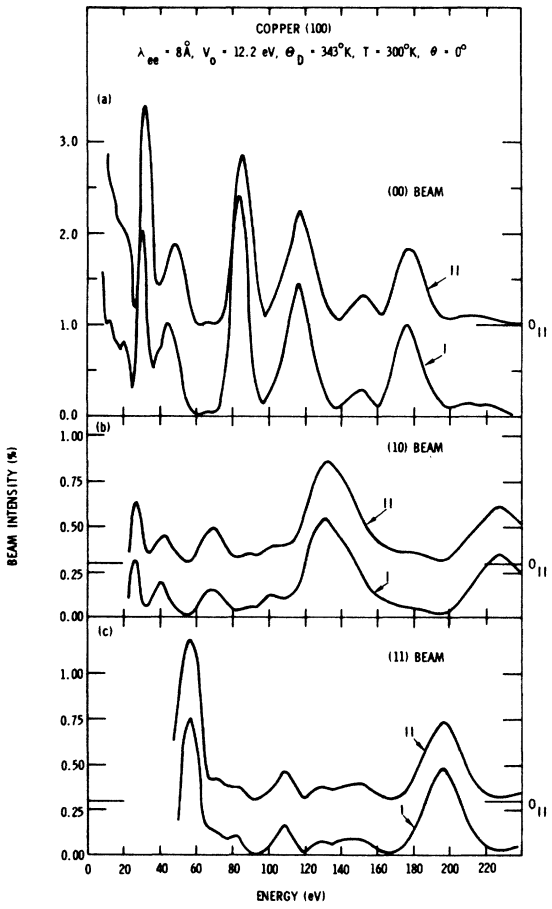

FIG. 2. Comparison between intensity profiles calculated using potential model I and potential model II. Both sets of curves are for the absolute reflectivities. The zero levels for the curves using potential model II have been shifted to the 1% mark for the specular beam and to the 0.3% mark for the (10) and (11) beams. The parameters indicated in the figure were used in both sets of calculations. The beams are indexed in terms of the primitive square lattice of the surface net.

shifts for this potential are shown as model II in Fig. 1.

Although the general qualitative behavior of the phase shifts is the same in both models, there are several noticeable quantitative differences. For example, in model I the d-wave resonance occurs at 4 eV and the s-wave resonance at 98 eV, while in model II the d-wave resonance occurs at 9 eV and the s-wave resonance at 88 eV relative to the respective muffin-tin zero levels. There are also distinct differences in the behavior of the p-wave components at the lower energies and in the behavior of the d-wave components in the middle-energy range.

These differences give rise to only inconsequential changes in the calculated LEED intensity profiles. This can be seen in Fig. 2 where intensity profiles calculated using the two different potential models are directly compared. The calculations are for a normally incident beam on Cu(100) and other than the different sets of phase shifts shown in Fig. 1, use exactly the same parameters, i.e. V_0, λ_{ee}, and Θ_D. The most noticeable difference between the two calculations occurs for the (00) beam at low-energies where more resolved structure occurs in the curves using model I. Also the ratios of the 31- and 46-eV peak intensities are somewhat different in the two models and there are some slight differences in the absolute peak intensities. The greatest discrepancy in peak positions occurs for the second of these two peaks which lies at 46 eV using model I and at 49 eV using model II. However, except for this one instance, the peak positions in all three beams agree within ~1 eV and the shapes of the peaks are quite comparable. Since these are presently the most important criteria in analyzing experimental LEED spectra, it was felt that it was immaterial as to which potential model was used. Because Snow and Waber's[10] band calculation indicates that potential model I is reasonably consistent with the low-lying electronic properties, it was decided to use it in the following LEED calculations. Nevertheless, the demonstrated adequacy of potential model II is important because of the ease with which it can be extended both to take account of specifically surface effects in clean metals[30] and also to adsorbate-substrate systems.[11]

As a further demonstration of the relative insensitivity of LEED to the details of the electron–ion-core potential, model calculations were performed using the self-energy and atomic geometry appropriate to copper in conjunction with the nickel–ion-core potential of Ref. 5. The curves for the (10) and (11) beams and for the (00) beam above 60 eV were virtually identical with the model II curves shown in Fig. 2. Below 60 eV in the (00) beam there were some minor differences in the absolute peak intensities but not in peak positions. The main differences between copper and nickel are in regards to their higher-lying electronic properties to which LEED is simply not sensitive.

III. COPPER (100)

In this section we compare calculated intensity profiles for Cu(100) with experimental measurements.[6–8] All calculations use $\lambda_{ee} = 8$ A as described earlier and unless otherwise stated, treat the surface as if it were simply a truncation of an idealized perfectly periodic bulk solid. Five atomic layers are treated in the calculations of this section. The 300 °K lattice constant (3.61 Å) is used and all beams are indexed according to the primitive square lattice of the surface net. The polar

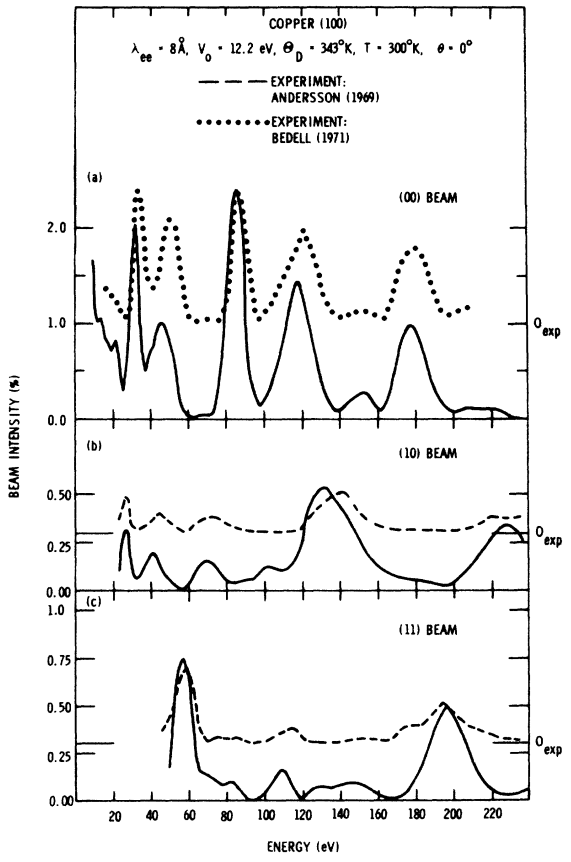

FIG. 3. Comparison between the predictions of the model calculations for a normally incident beam and the measurements of Bedell (Ref. 7) for the specular beam and the measurements of Andersson (Ref. 6) for the (10) and (11) beams. Both the theoretical calculations and the experimental measurements are for the absolute reflectivity. The experimental zero levels have been shifted to the 1% mark for the (00) beam and to the 0.3% mark for the (10) and (11) beams. The parameters used in the calculation are indicated in the figure.

angle θ is defined relative to the surface normal, and the azimuthal angle φ is defined relative to the (10) beam direction. The beam labeling convention and the definition of φ are explicitly shown in Fig. 1 of Ref. 5.

In Fig. 3 we compare model calculations at normal incidence with the experimental measurements of Andersson[6] and of Bedell.[7] The calculated specular beam shows excellent agreement with Bedell's[7] data. Below 25 eV the model calculation predicts a bit too much fine structure (the experimental measurement looks more like the model-II calculation shown in Fig. 2), but this is felt not to be a serious problem. Except for the peak structure between 120–160 eV, the (10) beam shows good agreement between theory and experiment. There is about a 10-eV discrepancy between the calculated and experimental positions of the actual maxima in this region. Such an effect can be due to the motion of a "Bragg envelope" over a multiple scattering structure and can be quite sensitive to small changes in the angle of incidence.[31] The (11) beam also exhibits fairly good agreement between theory and experiment. However, the predicted shape of the structure between 170–220 eV is a

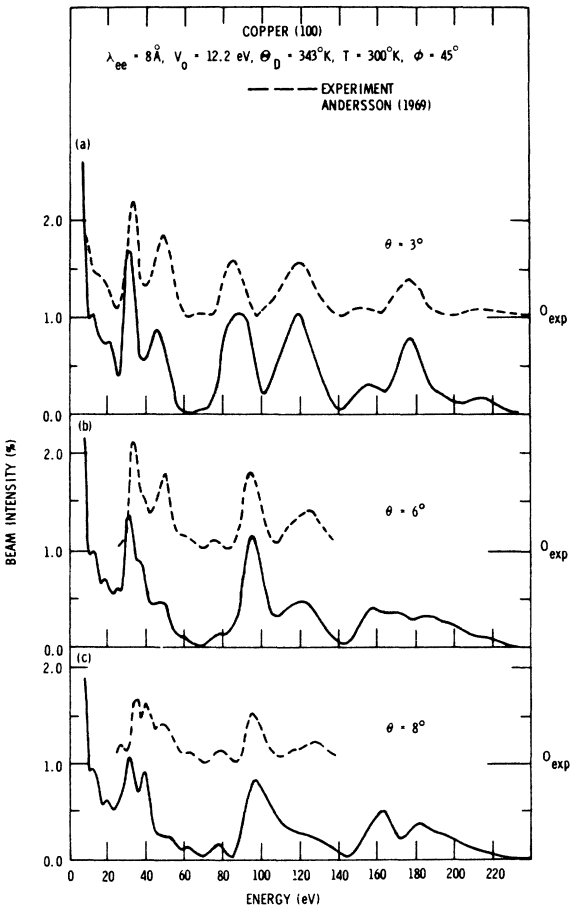

FIG. 4. Comparison between the predictions of the model calculations for the specular beam and the experimental measurements of Andersson (Ref. 6) for $\varphi = 45°$ and various polar angles. Panel (a) shows the curves for $\theta = 3°$, panel (b) shows the curves for $\theta = 6°$, and panel (c) shows the curves for $\theta = 8°$. Both the theoretical calculations and the experimental measurements are for the absolute intensities with the model calculations using the parameters indicated in the figure. The zero levels for the experimental measurements have been shifted to the 1% mark.

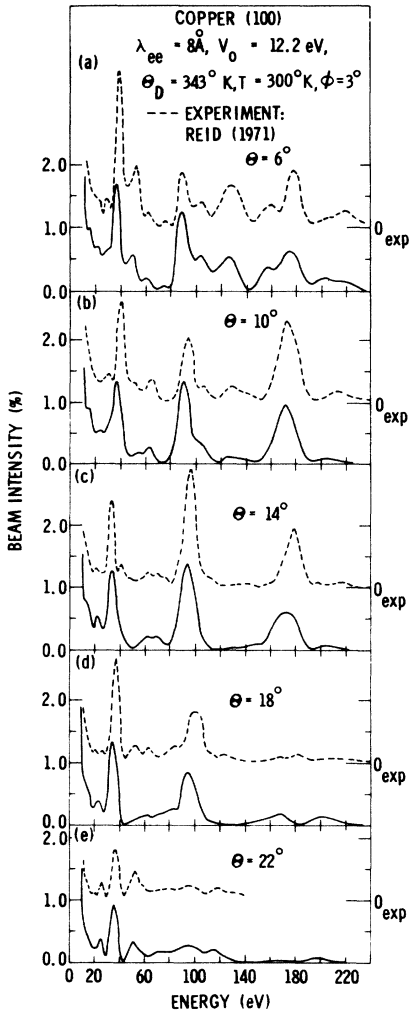

FIG. 5. Comparison between the predictions of the model calculations for the specular beam and the experimental measurements of Reid (Ref. 8) for $\varphi = 3°$. The curves are labeled by the polar angle θ. The theoretical calculations are for the absolute intensity but the experimental measurements are only of the relative intensity. The two sets of curves were normalized with respect to the 85-eV peak for $\theta = 6°$ and the experimental zero levels were shifted to the 1% mark. The parameters used in the calculation are indicated in the figure.

little off with the experiment showing a shoulder not seen in the model calculations. It could well be that the influence of the $l=5$ phase shift is important in this region and this could account for the discrepancy between theory and experiment. There is reasonable correspondence between the theoretical calculations and the experimental measurements as far as the magnitude of the absolute intensity. Using $\lambda_{ee}=11$ Å has the effect of scaling up the calculated curves by about a factor of 1.5 and so about all that one can actually say is that there is an order of magnitude agreement between the model calculations and the experimental measurements.

A comparison between the model calculations for the specular beam and the experimental intensity profiles of Andersson[6] for $\varphi=45°$ and various angles of incidence is shown in Fig. 4. For $\theta=3°$ there is good agreement between theory and experiment over the entire energy range. For $\theta=6°$ and 8° the experimental data extend only out to 140 eV. In both cases there is reasonable agreement between theory and experiment although there is a substantial peak in the experiment, whereas in the theory it appears as a shoulder or at best a relatively small peak. The splitting of the structure between 30–40 eV into a doublet as θ increases from 6° to 8° is well illustrated in the model calculations.

The above experimental data cover only a relatively narrow range of polar angles. The experimental data of Reid,[8] on the other hand, cover a much wider range. His measurements were not precisely along a symmetry direction but were at $\varphi=3°$. Figure 5 shows the comparison between his experimental measurements and the model calculations. The experimental measurements were for relative rather than absolute intensities and were normalized to the theoretical calculations at the 85-eV peak for $\theta=6°$. Except for the fine structure below 30 eV, the agreement between theory and experiment is quite good for $\theta=6°$ and 10°. For $\theta=14°$ there are noticeable differences between the experimental and theoretical curves and the degree of correspondence worsens further when θ is increased to 18°. Curiously, for $\theta=22°$ the agreement between theory and experiment, instead of deteriorating further, has improved with respect to the $\theta=18°$ curves. Since it seems likely that future experimental measurements will be at $\varphi=0°$ rather than $\varphi=3°$, an effort was made to ascertain how much the calculated curves would change on going to $\varphi=0°$. It was found that even for $\theta=22°$ there were no substantial changes in the shapes of the calculated curves and so it is felt that the calculated curves are repre-

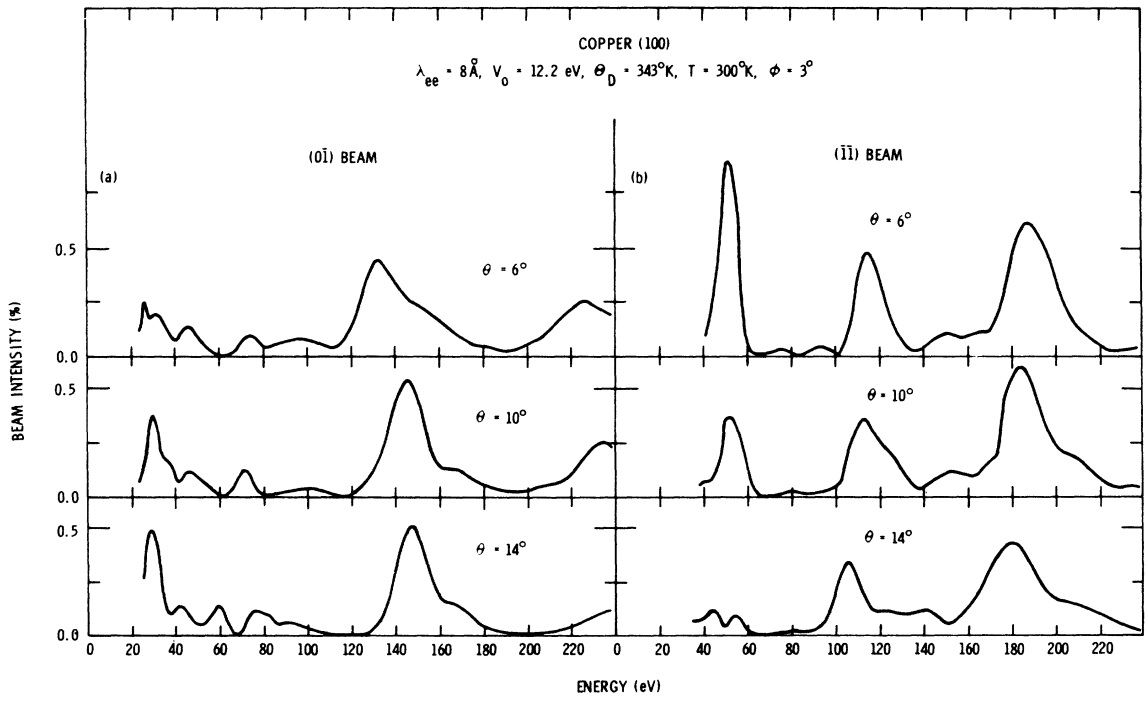

FIG. 6. Calculated intensity profiles for the (0$\bar{1}$) beam, panel (a), and the ($\bar{1}\bar{1}$) beam, panel (b), for $\varphi=3°$ and the indicated angles of incidence. The calculations are for the absolute intensity and use the parameters indicated in the figure.

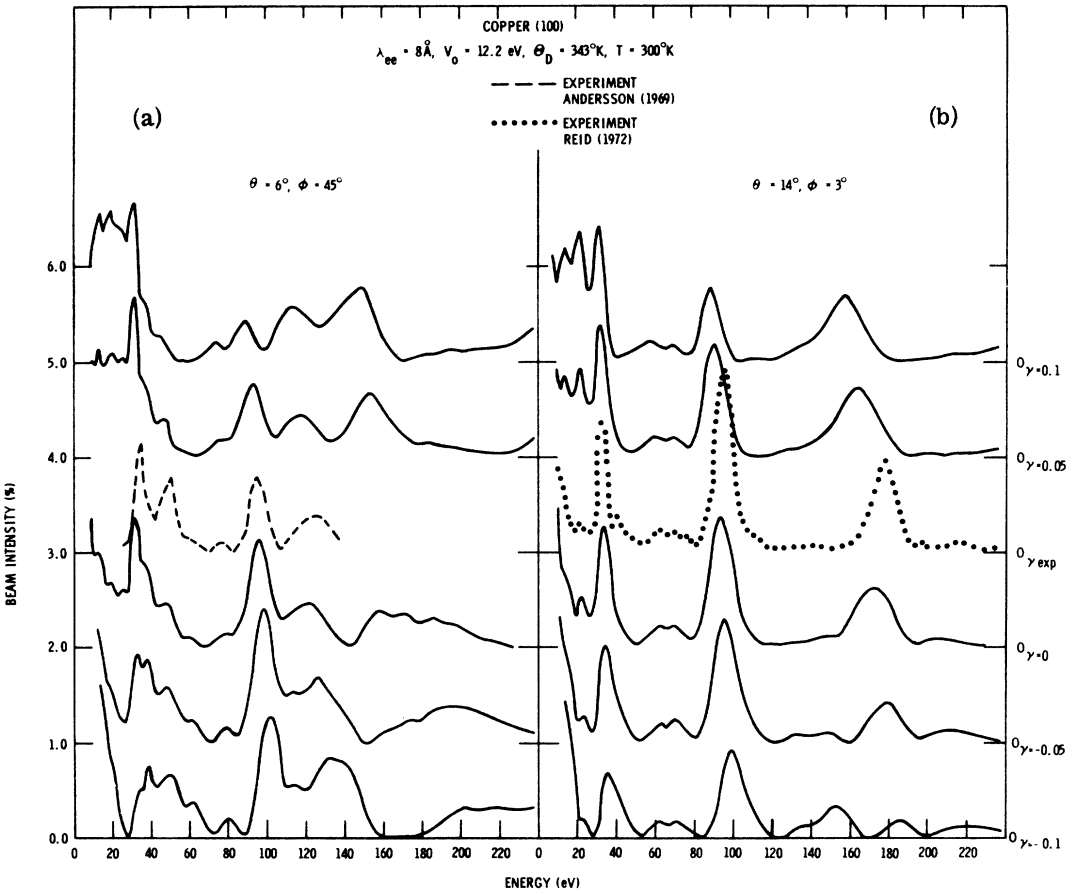

FIG. 7. Effect of a small change in the upper-layer spacing on the calculated intensity profiles. The calculations are for the specular beam at $\theta = 7°$, $\varphi = 45°$ in panel (a) and at $\theta = 14°$, $\varphi = 3°$ in panel (b). Also shown are the corresponding experimental measurements of Andersson (Ref. 6) and of Reid (Ref. 8). The theoretical curves are for the absolute intensity as is the experimental curve of Andersson. The measurement of Reid is for the relative intensity and has been normalized as discussed in the text. The zero level has been shifted to the 1% mark for $\gamma = -0.05$, to the 2% mark for $\gamma = 0$, to the 3% mark for the experimental curves, to the 4% mark for $\gamma = 0.05$, and to the 5% mark for $\gamma = 0.1$. The upper-layer spacing is defined in terms of γ through Eq. (6) of the text.

sentative of those for $\varphi = 0°$.

To help motivate additional experimental work, calculated intensity profiles for the $(0\bar{1})$ and $(\bar{1}\bar{1})$ beams are shown in Fig. 6 for $\varphi = 3°$ and $\theta = 6°$, 10°, and 14°. Using the inelastic-collision-model formalism the calculation of these additional beams for a given set of angles of incidence costs negligible computer time. Again we note there are no substantial changes in the curves on going from $\varphi = 3°$ to the more symmetrical $\varphi = 0°$.

The agreement between theory and experiment shown in Figs. 3–5, although not as good as obtained for nickel,[5] seems reasonably satisfactory. The question obviously arises as to whether this agreement can be improved by varying the upper-layer spacing used in the calculations. To investigate this we write the upper-layer spacing as

$$d' = (1 + \gamma)d \,, \tag{6}$$

where d is the bulk layer spacing of 1.805 Å and γ denotes the deviation from the bulk value. In Fig. 7 we show calculated curves for $\gamma = -0.1$, -0.05, 0, 0.05, and 0.1 and compare them with the experimental data. The particular angles of incidence shown were $\theta = 6°$, $\varphi = 45°$, and $\theta = 14°$, $\varphi = 3°$. These angles were chosen because of the difficulty in describing certain features of the experimental curves using $\gamma = 0$. For $\theta = 6°$, $\varphi = 45°$ the 50-eV peak was more pronounced in the experiment[6] than in the $\gamma = 0$ calculation. A contraction of the upper-layer spacing does enhance this peak in the calculated curves but severely disturbs the agreement between theory and experiment as far as other features are concerned. For $\theta = 14°$, $\varphi = 3°$ the experimental curve shows a small resolved peak above 40 eV but the $\gamma = 0$ calculation shows only a high-energy tail. A contraction of the upper-layer spacing enhances the high-energy

tail but does not produce a resolved peak.

In both instances a value of $\gamma = 0$ seems to provide a better over-all description of the experimental data than $\gamma \neq 0$. The effects of a change in the upper-layer spacing can clearly be seen for $\gamma = \pm 0.05$ and so we conclude that the upper-layer spacing for Cu(100) coincides with its bulk value to within $\pm 5\%$ or about 0.1 Å. Because of the intrinsic uncertainties in our model of the electron-solid force law,[3] it does not seem reasonable to try to push the model to a greater accuracy than this.

IV. COPPER (111)

In this section model calculations of LEED intensities from Cu(111) are performed and compared with experimental measurements.[7,8] As before, the nonspecular beams are indexed according to the primitive surface net and the azimuthal angle φ is defined relative to the direction of the (10) beam. The beam labeling convention and the definition of φ are explicitly shown in Fig. 1 of Ref. 5. Unless otherwise stated, the model calculations treat the surface as if it were a simple truncation of an idealized perfectly periodic bulk solid.

The calculations initially used $\lambda_{ee} = 8$ Å as was done in Sec. III. However, this value of λ_{ee} did not give a satisfactory description of the fine structure in the experimental intensity profiles. Using $\lambda_{ee} = 11$ Å provided a substantially better description of this fine structure. This is illustrated in Fig. 8 where we compare theoretical intensity profiles using $\lambda_{ee} = 8$ Å and 11 Å with the normal incidence, specular-beam measurements of Bedell.[7] Calculations are also shown for the (10) and $(\bar{1}0)$ beams. Comparing the model calculation using $\lambda_{ee} = 8$ Å with Bedell's[7] experimental mea-

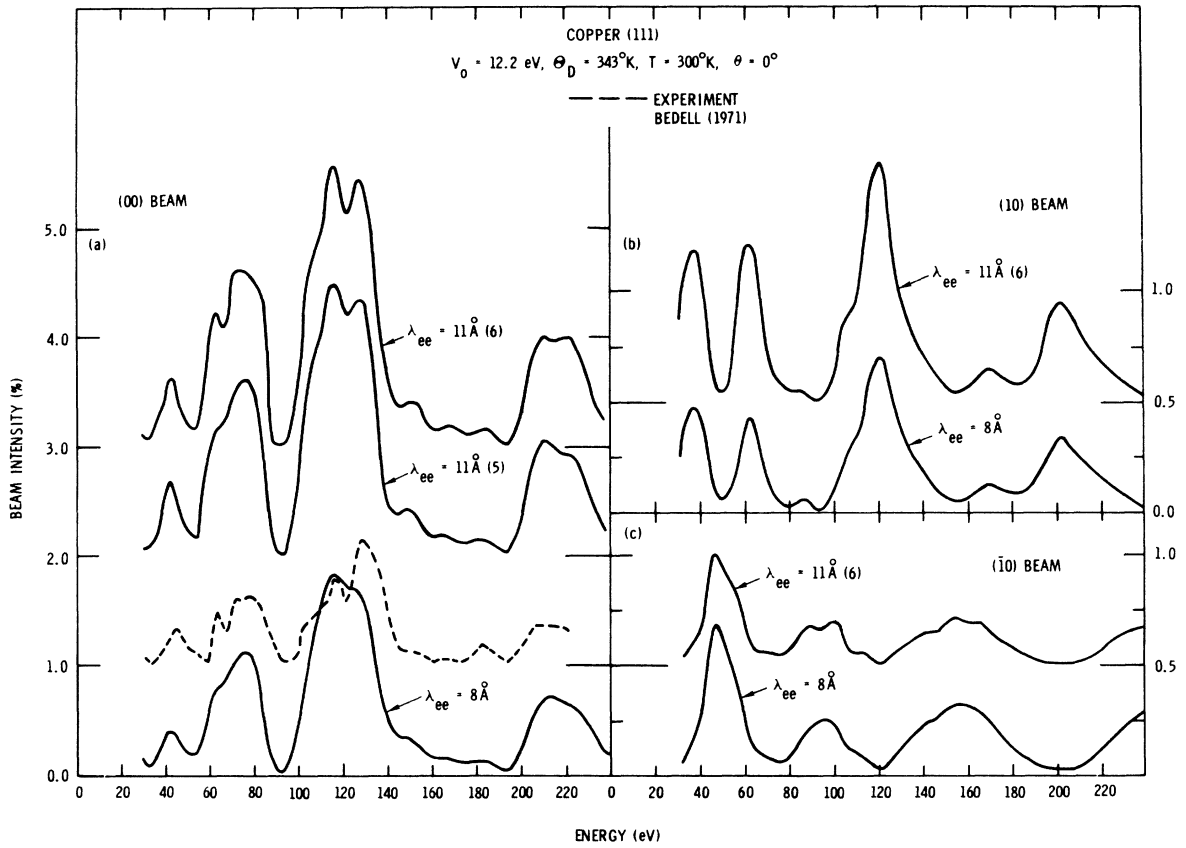

FIG. 8. Comparison between calculated intensity profiles using $\lambda_{ee} = 8$ A and $\lambda_{ee} = 11$ Å and the experimental measurements of Bedell (Ref. 7). The theoretical curves labeled $\lambda_{ee} = 11$ Å (6) were calculated using six atomic layers and the curves labeled $\lambda_{ee} = 11$ Å (5) were calculated using five atomic layers. The curves in panel (a) are for the (00) beam, in panel (b) are for the (10) beam, and in panel (c) are for the $(\bar{1}0)$ beam. Both the theoretical calculations and the experimental measurements are for the absolute intensities. For the (00) beam the zero level has been shifted to the 1% mark for the experimental curve, to the 2% mark for the $\lambda_{ee} = 11$ Å (5) curve, and to the 3% mark for the $\lambda_{ee} = 11$ Å (6) curve. For both the (10) and $(\bar{1}0)$ beams the zero level has been shifted to the 0.5% mark for the $\lambda_{ee} = 11$ Å (6) curve. The other parameters used in the calculation are shown in the figure.

surement, we see that the calculation reproduces the gross structure but misses a lot of the fine structure on the peaks. This effect is often indicative of using too small a value of λ_{ee}. To check this the calculation was redone using $\lambda_{ee} = 11$ Å and five atomic layers. The results of this calculation are shown as the curve labeled $\lambda_{ee} = 11$ Å (5). The major effect is a change in the over-all scale of the curve with there being some minor changes in peak shapes. However, for adequate convergence in the calculations we expect that we must have

$$nd \gtrsim \lambda_{ee} \ , \tag{7}$$

where d is the layer spacing and n is the number of layers used in the calculations. For Cu(111), $d = 2.08$ Å; and so although five atomic layers are sufficient for $\lambda_{ee} = 8$ Å, we must use at least six atomic layers for $\lambda_{ee} = 11$ Å. Results of model calculation using six atomic layers are shown as the curves labeled $\lambda_{ee} = 11$ Å (6). Note the significant changes in the details of the fine structure and the peak shapes on going to six layers and the improved agreement with experiment. Ideally, we would like to check the convergence by doing the calculation with still more layers (as was done in checking the convergence of the $\lambda_{ee} = 8$ Å, five layer calculations), but six atomic layers are the limit of the present computer code if five partial-wave components are used to describe the electron–ion–core scattering amplitude.[32] Apart from the fact that six layers satisfy Eq. (7), the degree of correspondence between theory and experiment is a reasonable indication that the calculation is fairly well converged.

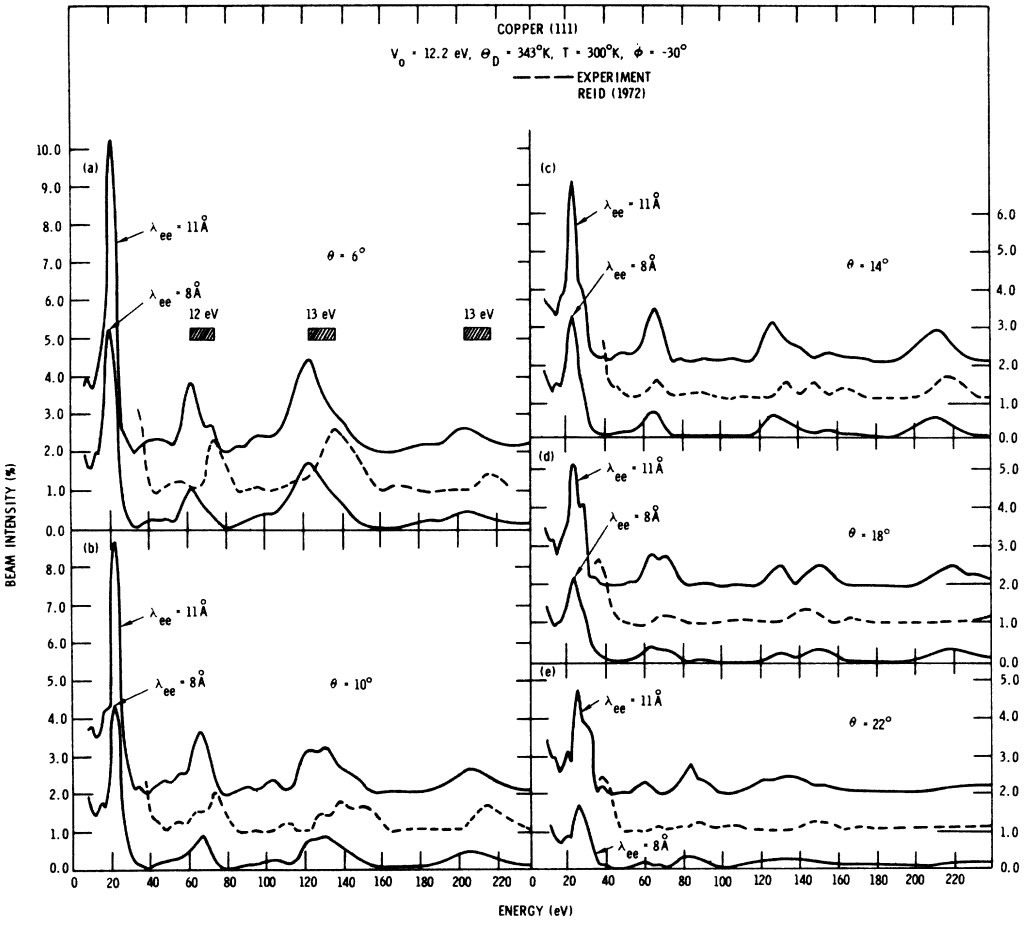

FIG. 9. Comparison between the predictions of the model calculations for the specular beam and the experimental measurements of Reid (Ref. 8) for $\varphi = -30°$. The curves are labeled by the polar angles θ. The theoretical curves were calculated using both $\lambda_{ee} = 8$ Å and $\lambda_{ee} = 11$ Å and are labeled accordingly. The other parameters used in the calculation are indicated in the figure. The theoretical curves are for the absolute intensity but the experimental curves are only for the relative intensity and have been normalized as discussed in the text. The zero level has been shifted to the 1% mark for the experimental curves and to the 2% mark for the theoretical calculations using $\lambda_{ee} = 11$ Å.

Upon realizing that $\lambda_{ee} = 11$ Å was probably closer to reality for copper than $\lambda_{ee} = 8$ Å, selected calculations were redone for Cu(100) using $\lambda_{ee} = 11$ Å and six atomic layers. Other than about a 40% over-all increase in the calculated intensity, there was little change in the curves—i.e., there were negligible changes in the details of the fine structure. This indicates that the calculated intensity profiles for Cu(111) are more sensitive to the value of λ_{ee} than those for Cu(100). Presumably this is due to the different packing sequence of the layers and this would hold for other fcc materials as well. The ~40% increase in the magnitude of the calculated intensities on going from $\lambda_{ee} = 8$ Å to $\lambda_{ee} = 11$ Å means that the calculated absolute intensities are larger than the experimental absolute intensities. However, there is still agreement to within a factor of ~2 and this is quite reasonable in view of the highly simplified models used for both the electron-solid force law and the surface topography. Because of the relatively minor changes that occurred for the Cu(100) curves it was not felt worthwhile to redo the figures using $\lambda_{ee} = 11$ Å.

Panels (b) and (c) of Fig. 8 show the changes in two nonspecular beams for the (111) surface on going from $\lambda_{ee} = 8$ Å to $\lambda_{ee} = 11$ Å. There is only an over-all scale factor change for the (10) beam, but the $(\bar{1}0)$ beam shows a significant change in the fine structure as well. In the Ni(111) calculations,[5] a value of 8Å was used for λ_{ee} and it was noticed that experimental fine structure in the $(\bar{1}0)$ and $(\bar{2}0)$ beams was lacking in the model calculations. Preliminary investigations show that using a value of 11 Å for λ_{ee} greatly improves the description of the fine structure in the Ni(111) calculations indicating that $\lambda_{ee} = 11$ Å is reasonable for both copper and nickel.

In Fig. 9 we compare model calculations for the specular beam for various angles of incidence with the experimental measurements of Reid.[8] The model calculations were performed using both $\lambda_{ee} = 8$ Å and $\lambda_{ee} = 11$ Å, with six atomic layers being used in the $\lambda_{ee} = 11$ Å calculations. The experimental measurements were for $\varphi = -30°$. By symmetry the (00) beam for this azimuth is the same as for any direction bisecting adjacent beams in the $\{10\}$ star. The experimental measurements are for relative rather than absolute intensity and were normalized to the theoretical calculations using $\lambda_{ee} = 8$ Å at the 140-eV peak for $\theta = 6°$. The most dramatic feature shown in the figure is that the experimental curves appear to be shifted about 13 eV higher in energy than the theoretical curves. This offset is shown explicitly in panel (a). This shift is extremely puzzling since the same value of $V_0 = 12.2$ eV was used in these calculations as was used previously. This value of V_0 gave a good description of all the experimental data[6–8] on Cu(100) and of Bedell's Cu(111) measurements.[7] The agreement between theory and experiment is quite acceptable for $\theta = 6°$ and 10° if this shift is taken into account. However, for $\theta \geq 14°$ even with this shift the agreement has markedly deteriorated. We also note that going to $\lambda_{ee} = 11$ Å has made a significant improvement in the description of the fine structure for $\theta = 10°$.

To obtain limits on the upper-layer spacing for Cu(111) we return to Bedell's[7] normal incidence measurements of the (00) beam. Calculations were performed using various values of the upper-layer spacing and these are compared with experiment in Fig. 10. The upper-layer spacing is defined in terms of γ through Eq. (6) of the text where

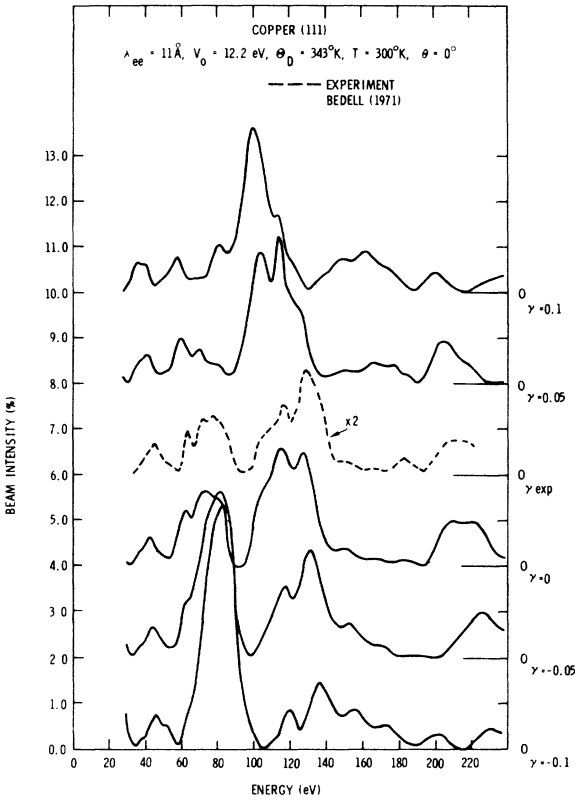

FIG. 10. Effect of a small change in the upper-layer spacing on the calculated intensity profiles for the specular beam. Also shown are the experimental data of Bedell (Ref. 7). Both the theoretical and the experimental curves are for the absolute intensity but the experimental curve has been multiplied by 2 to facilitate comparison with the model calculations. The zero level has been shifted to the 2% mark for $\gamma = -0.5$, to the 4% mark for $\gamma = 0$, to the 6% mark for the experimental curve, to the 8% mark for $\gamma = 0.05$, and to the 10% mark for $\gamma = 0.1$. The upper-layer spacing is defined in terms of γ through Eq. (6) of the text. The model calculations use the parameters indicated in the figure.

and ($\bar{1}0$) beams. Comparing the model calculation using $\lambda_{ee} = 8$ Å with Bedell's[7] experimental mea- $d = 2.08$ Å for Cu(111) at 300 °K. Bedell's experimental data have been multiplied by a factor of two to facilitate comparison with the model calculations. Six atomic layers were used in these calculations. As far as peak shapes and positions are concerned, for the regions between 30–100 eV and 180–220 eV the best agreement with experiment is for $\gamma = 0$. However, for the region between 100–160 eV the agreement with experiment is clearly the best for $\gamma = -0.05$. The comparison with experiment definitely appears to rule out any significant expansion of the upper-layer spacing but is unable to rule out a slight contraction. Because ± 5% is felt to be the intrinsic accuracy of this procedure, it seems most reasonable to simply state that the upper-layer spacing of Cu(111) equals its bulk value to within about 5% or ~0.1 Å.

V. SUMMARY AND CONCLUSIONS

In this paper the finite temperature version[1–5] of the inelastic collision model was used to analyze room-temperature experimental LEED intensity profiles[6–8] for Cu(100) and Cu(111). Two models of the electron–ion-core potentials were compared—a self-consistent band-structure potential[10] and a potential constructed from a simple overlap of atomic charge densities. It was found that the differences in the calculated intensity profiles using these two different model potentials were negligible as far as analyzing experimental LEED data. It was observed previously that a potential constructed from overlapping atomic charge densities worked well for LEED calculations for nickel,[5] but because of the different electronic properties of nickel and copper, it was felt worthwhile to show this directly. The inner potential used in the calculations was obtained by comparing Snow and Waber's[10] energy-band calculations with experimental work function measurements for polycrystalline copper.[12,13] Except for one set of experimental data on Cu(111), this value of V_0 gave a good fit to experimental peak positions. The discrepancy for Reid's specular-beam data[8] on Cu(111) could well be due to experimental difficulties although this is by no means certain. Even in this case the discrepancy between theory and experiment was in the nature of a constant offset and so it is felt that the inner potential exhibits no significant variation over the energy range considered.

A constant inelastic mean-free-path parameter was used in the calculations. The model calculations performed initially were for Cu(100) and used $\lambda_{ee} = 8$ Å. This gave a good description of the shapes of both the shapes and the absolute intensities of the experimental intensity profiles. However, on turning to Cu(111), it was found that this value of λ_{ee} did not give a satisfactory description of the fine structure in the calculated profiles. λ_{ee} was then increased to 11 Å and the fine structure in the calculated curves was much improved. Selected calculations were then redone for Cu(100) using $\lambda_{ee} = 11$ Å, and it was found that apart from an over-all scale increase of order 40–50%, there was little change in the calculated profiles. Because of this, it was not felt worthwhile to redo the Cu(100) calculations. Even with this scale increase, the calculated absolute intensities agree with the experimental measurements to within a fraction of 2 or 3,. and this is in keeping with the simplicity of the model. We conclude that the fine structure in the calculated intensity profiles from Cu(111) is much more sensitive to the value of λ_{ee} than that in the calculated profiles for Cu(100). Preliminary investigations show that it is also true for nickel. Hence it would appear advisable in future work to check the value of λ_{ee} through calculations on the (111) face of an fcc material before embarking on detailed calculations for the other faces. Of course, it would be advantageous to determine λ_{ee} without having to make subjective judgments about the degree of fit between the calculated and measured intensity profiles. If one knew independently the vibrational amplitude of the atoms in the surface region, then λ_{ee} (E) could be determined from the temperature dependence of the scattered intensity.[33] Looking at the total integrated (in angle) elastically scattered intensity would eliminate the vibronic effects and minimize the effects of surface morphology,[34] and hence one should be able to determine λ_{ee}(E) by directly comparing the calculated integrated elastic intensity for a perfect rigid lattice with experimental measurements. Preliminary work on silver by Jona *et al.*[35] indicates that this approach is feasible.

Calculations were performed with different values of the upper-layer spacing and the results compared with experiment. The best fit for Cu(100) was obtained when the upper-layer spacing equaled the bulk value. In the case of Cu(111) some features of the calculated curves agreed best with experiment when the upper-layer spacing equaled the bulk value and some features agreed best for a slightly contracted upper-layer spacing. For both faces it is felt that to within about 5% or ~0.1 Å the upper-layer spacing equals the bulk value.

ACKNOWLEDGMENT

I would like to thank D. G. Schreiner for his assistance in plotting the experimental data.

*Work supported by the U. S. Atomic Energy Commission.

[1]C. B. Duke and G. E. Laramore, Phys. Rev. B 2, 4765 (1970).
[2]G. E. Laramore and C. B. Duke, Phys. Rev. B 2, 4783 (1970).
[3]G. E. Laramore and C. B. Duke, Phys. Rev. B 5, 267 (1972).
[4]C. B. Duke, D. L. Smith, and B. W. Holland, Phys. Rev. B 5, 3358 (1972).
[5]G. E. Laramore, Phys. Rev. B 8, 515 (1973).
[6]S. Andersson, Surf. Sci. 18, 325 (1969).
[7]L. R. Bedell, Ph.D. thesis (Brown University, 1971) (unpublished); L. R. Bedell and H. E. Farnsworth, Surf. Sci. 41, 165 (1974).
[8]R. J. Reid, Surf. Sci. 29, 603 (1972).
[9]R. J. Reid, Phys. Status Solidi A 4, K211 (1971); Surf. Sci. 29, 623 (1972).
[10]E. C. Snow and J. T. Waber, Phys. Rev. 157, 570 (1967).
[11]C. B. Duke, N. O. Lipari, G. E. Laramore, and J. B. Theeten, Solid State Commun. 13, 579 (1973).
[12]E. W. J. Mitchell and J. W. Mitchell, Proc. R. Soc. A 210, 70 (1951).
[13]J. C. Riviere, Proc. Phys. Soc. Lond. B 70, 676 (1957).
[14]C. B. Duke and C. W. Tucker, Jr., Phys. Rev. Lett. 23, 1163 (1969); Surf. Sci. 15, 231 (1969).
[15]G. E. Laramore, C. B. Duke, A. Bagchi, and A. B. Kunz, Phys. Rev. B 4, 2058 (1971).
[16]J. B. Pendry, J. Phys. C 4, 2514 (1971).
[17]J. B. Pendry, *LEED: Surface Structure of Solids* (Union of Czechoslovak Mathematicians and Physicists, Prague, 1972), Vol. 2, p. 305.
[18]D. W. Jepsen, P. M. Marcus, and F. Jona, Phys. Rev. B 5, 3973 (1972).
[19]P. M. Marcus, D. W. Jepsen, and F. Jona, Surf. Sci. 31, 180 (1972).
[20]G. A. Burdick, Phys. Rev. 129, 138 (1963).
[21]S. Andersson and B. Kasemo, Surf. Sci. 25, 273 (1971).
[22]This is the value of Θ_D used in Ref. 21. Experimental values of Θ_D in the bulk range from 344°K, based upon measurements of elastic constants, to 307°K, based upon x-ray-diffraction measurements. See, for example, Table II of R. H. Herbstein, Adv. Phys. 10, 313 (1961). The exact value of Θ_D does not appear critical to the present work which considers only room-temperature data.
[23]C. B. Duke, N. O. Lipari, and U. Landman, Phys. Rev. B 8, 2454 (1973).
[24]B. W. Holland, Surf. Sci. 28, 258 (1971).
[25]G. E. Laramore and A. C. Switendick, Phys. Rev. B 7, 3615 (1973).
[26]D. Liberman, J. T. Waber, and D. T. Cromer, Phys. Rev. 137, A27 (1965).
[27]T. Loucks, *Augmented Plane Wave Method* (Benjamin, New York, 1967).
[28]J. C. Slater, Phys. Rev. 81, 385 (1951).
[29]W. Kohn and L. J. Sham, Phys. Rev. 140, A1133 (1965).
[30]J. E. Houston, R. L. Park, and G. E. Laramore, Phys. Rev. Lett. 30, 846 (1973).
[31]C. W. Tucker, Jr. and C. B. Duke, Surf. Sci. 24, 31 (1971).
[32]The trade off between partial-wave components and the number of atomic layers is discussed by S. Y. Tong, G. E. Laramore, and T. N. Rhodin, Phys. Rev. B (to be published).
[33]G. E. Laramore, Phys. Rev. B 6, 1097 (1972).
[34]G. E. Laramore, J. E. Houston, and R. L. Park, J. Vac. Sci. Technol. 10, 196 (1973).
[35]F. Jona (private communication).